Annals of Biomedical Engineering, Vol. 39, No. 1, January 2011 *(© 2010)* pp. 414–426
DOI: 10.1007/s10439-010-0151-y

Influences of Acid-Treated Multiwalled Carbon Nanotubes on Fibroblasts: Proliferation, Adhesion, Migration, and Wound Healing

YUYING ZHANG, BING WANG, XINAN MENG, GUANQING SUN, and CHANGYOU GAO

MOE Key Laboratory of Macromolecular Synthesis and Functionalization, Department of Polymer Science and Engineering, Zhejiang University, Hangzhou 310027, China

(Received 24 May 2010; accepted 20 August 2010; published online 8 September 2010)

Associate Editor Mona Kamal Marei oversaw the review of this article.

Abstract—With the increasing applications of carbon nanotubes (CNTs) in fields of biomedical engineering and medical chemistry, it is important to understand the response of mammalian cells to the CNTs exposure and treatment. In this study, the influences of multiwalled carbon nanotubes (MWCNTs) on cellular behavior of human dermal fibroblasts and NIH 3T3 murine fibroblasts were investigated. Results showed that the MWCNTs treatment induced dose-dependent cytotoxicity and arrested the cell cycle in the G1 phase, indicating inhibition of DNA synthesis. The presence of MWCNTs also down regulated the expression level of adhesion-related genes, and simultaneously caused cytoskeleton damage and disturbance of actin stress fibers, thereby inducing dramatically adverse effects on the cell physiological functions such as cell spreading, adhesion, migration, and wound healing ability.

Keywords—Carbon nanotubes, Fibroblasts, Cell cycle, Adhesion, Migration.

INTRODUCTION

Carbon nanotubes (CNTs) comprised of cylinders of one or several graphite layers were first reported by Oberlin *et al.*[30] in 1976 and described in detail by Iijima[16] in 1991. As a class of stiff, stable, and hollow nanomaterials with many unique physical, chemical, and mechanical properties, the CNTs have being broadly used as nanowires, electronic components, catalyst supports, and recently extended to fields of biomedical engineering and medical chemistry.[1,2] For example, the CNTs may function as scaffolds for bone growth[50] and neuronal growth.[15] CNT–ligand conjugates can be taken up by special cell types and used to deliver drug or bioactive molecules, which is highly prospective in gene or peptide storage and delivery in molecular therapy of diseases.[11,23] As an atomic force microscopy tip, the CNTs also have been used to image biological molecules such as DNA and proteins with atomic resolution.[14]

However, the excellent properties that make the CNTs interesting also raise concerns about their potential adverse effects on biological systems, which may lead to health issues.[20,45] Particularly, with the increasing interest of the CNTs applications in biomedical research, it has become a focus to investigate the influences of CNTs and associated nanomaterials on human cells and environment. Actually, a large number of *in vitro* studies have demonstrated that both single walled carbon nanotubes (SWCNTs) and multiwalled carbon nanotubes (MWCNTs) can induce cytotoxicity in different cell types.[3,7,8,17,18,22,26,28,29,40,45,46] For example, it is found that the SWCNTs inhibit the proliferation of both HEK 293 cells[7] and human fibroblasts[46] through inducing cell apoptosis and decreasing cellular adhesive ability. Compared with activated carbon, the SWCNTs cause more severe inhibition of growth of smooth muscle cells.[37] The MWCNTs also induce a concentration- and time-dependant decrease in mitochondrial metabolism of human pulmonary cells[45] and cause oxidative stress in HEK 293 cells.[38] In order to reveal the molecular mechanism of cytotoxicity, Ding *et al.* performed whole genome expression array analysis on human skin fibroblasts and found that the genes involved in cellular transport, metabolism, cell cycle regulation, and stress response were activated after MWCNTs exposure.[8] A recent study reported that the SWCNTs damaged the actin cytoskeleton organization and

Address correspondence to Changyou Gao, MOE Key Laboratory of Macromolecular Synthesis and Functionalization, Department of Polymer Science and Engineering, Zhejiang University, Hangzhou 310027, China. Electronic mail: cygao@mail.hz.zj.cn

affected cell spreading,[19] suggesting that besides proliferation inhibition, the SWCNTs can induce impairment of certain vital cell functions. However, some contradictory results are also reported, revealing non-toxicity of the CNTs.[34] Particularly, to our best knowledge the influences of the MWCNTs on important cellular physiological events such as cell adhesion and migration have not been well documented.

It is known that the cell adhesion is of crucial importance in governing a variety of cellular functions including cell growth, migration, proliferation, differentiation, and tissue organization. Moreover, as one of the most important physiological processes of organisms, cell migration orchestrates embryonic morphogenesis, contributes to tissue repair and regeneration, and drives disease progression in cancer, mental retardation, atherosclerosis, and arthritis.[39] Therefore, in this study, human dermal fibroblasts from primary cultures and NIH 3T3 murine fibroblasts are used as the *in vitro* models to explore their interactions with the MWCNTs in terms of cell proliferation, adhesion, migration, change of wound healing ability and cytoskeleton organization. The CNTs both used in the biomedical field and exist in environment may cross through the skin or open wounds and contact with fibroblasts, which play an important role in the cell renewing system and wound repair process.[41] Thus, investigating the change of cell adhesion and migration abilities can further unveil the physiological side effects brought by the cellular uptake of the MWCNTs, which are usually neglected before.

MATERIALS AND METHODS

MWCNTs

The MWCNTs prepared by the method of chemical vapor deposition[25] were kindly offered by Prof. Xiaobin Zhang of Department of Materials Science and Engineering, Zhejiang University. They were purified according to the procedures described previously.[37] In brief, the MWCNTs were sonicated in a 3:1 (v/v) mixture of H_2SO_4 and HNO_3 for 30 min, refluxed for 6 h and then sonicated for another 30 min. The MWCNTs–acid mixture was cooled to room temperature, diluted with a large amount of deionized water and filtered through a 0.45 μm filter (Millipore, USA) to remove any residual acid. The treated MWCNTs was washed to neutral and re-suspended from the filter membrane into fresh water under sonication. The aqueous suspension was centrifuged at 5000 rpm for 5 min and the supernatant was decanted to remove any large impurities. The suspension containing only the finely dispersed MWCNTs were then lyophilized and used throughout this work.

The size and morphology was characterized with a JEM-200 transmission electron microscope (TEM, JEOL, Japan) and a ULTRA-55 scanning electron microscope (SEM, ZEISS, Germany). The average hydrodynamic size and zeta potential of the MWCNTs in aqueous solution were determined by dynamic light scattering (DLS) and electrophoretic movement using a Delsa^{TM} Nano zeta potential and submicron particle size analyzer (Beckman Coulter, USA), respectively. The residues of metallic impurities were analyzed by an atomic absorption spectrophotometer (Hitachi, Japan). The Fourier transform infrared (FT-IR) spectra were recorded on a Vector 22 FT-IR spectrophotometer (Bruker Optics, Switzerland).

Cell Culture

Primary human dermal fibroblasts were obtained from spare skin tissues with agreement of patients and were used between passages 5 and 13 in this study. Cell line NIH 3T3 murine fibroblast was obtained from American Type Culture Collection (ATCC, USA). The cells were maintained in regular growth medium consisting of high-glucose DMEM (Gibco, USA) supplemented with 10% fetal bovine serum, 100 U/mL penicillin, and 100 μg/mL streptomycin at 37 °C in a 5% CO_2 humidified environment. To make the results more close to the physiological conditions, the MWCNTs were suspended in growth medium supplemented with 10% serum in all the cell relevant experiments. Sonication of the MWCNTs containing medium was performed to ensure good dispersion before use.

Cell Viability Assay

The influences of the MWCNTs on the cell viability was assessed using the 3-[4,5-dimethylthiazol-2-yl]-2, 5-diphenyltetrazolium bromide (MTT) assay. Briefly, 10^4 fibroblasts in 100 μL medium were seeded into a well of a 96-well plate and incubated overnight. Then, the cells were treated in triplicate with MWCNTs of variable concentrations (weight/volume of solution): 1, 5, 10, 20, 50, and 100 μg/mL for 24 h, and maintained in fresh medium containing 0.5 mg/mL of MTT for another 4 h at 37 °C. The dark blue formazan crystals generated by the mitochondria dehydrogenase were dissolved with 150 μL dimethyl sulfoxide. 100 μL solution from each well was added into a new 96-well plate and measured at 570 nm using a MODEL 550 microplate reader (Bio Rad, USA). The data were normalized to the control group.

Flow Cytometric Analysis of the Cell Cycle

After treated with desired concentrations of MWCNTs for 24 h, the human dermal fibroblasts and NIH 3T3 fibroblasts were washed with phosphate buffered saline (PBS) thoroughly, and then harvested by trypsin treatment and fixed by incubation with cold 75% ethanol for 24 h. The fixed cells were then washed with PBS and incubated with staining solution (20 μg/mL propidium iodide, 100 μg/mL RNase-A in PBS) for 30 min. Flow cytometric measurement was performed on a FACS Calibur flow cytometry (Becton-Dickinson, USA). For each analysis, 10,000 events were monitored.

Cell Adhesion Assay and Real-Time RT-PCR Analysis

The cells were seeded on a 6-well plate at a density of 3×10^5 cells per well and cultured for 24 h. After treated with the MWCNTs of variable concentrations for 24 h, the cells were washed with PBS and detached with 0.25% trypsin, kept separated, and then placed on a 24-well plate at a density of 5×10^4 per well and allowed to adhere for another 24 h. The MWCNTs untreated cells were used as control. The morphologies of the cells were observed by using an optical microscope (Axovert 200, Carl Zeiss, Germany). After the non-adherent cells were removed by washing with PBS for three times, the adherent cells were quantitated by counting in 12 different areas under the optical microscope. The assays were repeated twice and each sample was assayed in triplicate. Data were averaged and normalized to the control.

Real-time quantitative reverse transcription polymerase chain reaction (real-time RT-PCR) was performed to examine the expression profiles of adhesion specific genes, i.e., fibronectin, laminin, and focal adhesion kinase (FAK) in human dermal fibroblasts. The fibroblasts were treated with 50 μg/mL MWCNTs for 24 h. The total RNA was extracted by using Trizol reagent (Invitrogen, USA) according to the manufacturer's instructions and quantified by using a biophotometer (Eppendorf, Germany). Total RNA samples (2 μg each) were used for reverse transcription under standard conditions using M-MLV Reverse Transcriptase cDNA synthesis kit (Promega, USA). The resulted cDNA was used as template in the subsequent PCR amplifications. The primer sequences used in this study are listed in Table 1. Glyceraldehyde-3-phosphate dehydrogenase (GAPDH) was used as endogenous reference housekeeping gene. The real-time PCR reactions were performed with the SYBR Premix Ex-Taq^{TM} Kit (Takara, Japan) and iQ^{TM} qPCR system (Bio Rad, USA). The relative gene expression values were calculated with the comparative $\Delta\Delta C_T$ (threshold cycle) method, as normalized to the housekeeping gene. The data were normalized to those of the cells cultured without the MWCNTs.

TABLE 1. Primer sequences for fibronectin, laminin, FAK, and GAPDH.

Gene	Primer sequence
Fibronectin	5′-CCTGGCACTTCTGGTCAGCAAC-3′
	5′-CCTACATTCGGCGGGTATGGTC-3′
Laminin	5′-CACCTATGTGCGTCTCAAGTTCC-3′
	5′-GCTGCTCGTCCCCTCCTGT-3′
FAK	5′-CTCCTGGTGCAATGGAGCGAGTAT-3′
	5′-GCAGGTGACTGAGGCGGAATC-3′
GAPDH	5′-CTGCTCCTCCTGTTCGACAGT-3′
	5′-CCGTTGACTCCGACCTTCAC-3′

Transwell Assay

The cell migration assay was carried out according to literature with some modifications.[42] Briefly, after treated with 20 μg/mL of MWCNTs for 24 h, the fibroblasts were washed with PBS, detached, and then 5×10^4 cells were suspended in DMEM containing 1% FBS and seeded into a Millicell (8-μm pores; Greiner Bio-One, Germany) which was mounted into a well of a 24-well plate in prior. 600 μL of the DMEM culture medium containing 20% FBS was added to the culture well. The cells were allowed to migrate for 10 h at 37 °C and 5% CO_2. After stained with 0.1% crystal violet, the migrated clones were photographed under an optical microscope. The cell number was counted at 12 different areas. Data were averaged from three parallel experiments, which were normalized to that of the control.

Wound Healing Assay and F-Actin Staining

The 70–80% confluent cells were treated with MWCNTs of variable concentrations for 24 h, and then scraped with a pipette tip to create a linear wound. The culture wells were washed twice with PBS and incubated with fresh regular medium. The wound closure of cells was observed and photographed using an optical microscope after 24, 48 and 72 h, respectively. The assays were repeated twice and each sample was assayed in triplicate. In order to observe the wound healing process more clearly, fluorescein diacetate (FDA), a live cell indicator, was added to monitor the cells by fluorescence microscopy. The images were analyzed by Image J software to obtain the quantitative data of the wound healing degree.

For staining cellular F-actin, 24 h after wounding, the fibroblasts were washed twice with PBS, fixed with 4% paraformaldehyde for 30 min, and then

permeabilized with 0.5% Triton X-100 at 4 °C for 5 min, then incubated at 37 °C for 30 min in 1% BSA/PBS to block non-specific bindings. The cells were subsequently treated with 0.15 μM rhodamine-conjugated phalloidin (Molecular Probes, USA) for 20 min and the nuclei were stained by incubation with 2 μg/mL DAPI dye (Sigma, USA) for 10 min at room temperature in dark.

Statistic Analysis

Results are reported as mean ± SD. Data were analyzed using t test for differences. The significant level was set as $p < 0.05$.

RESULTS

Characterization of MWCNTs

As illustrated in Fig. 1a, the pristine MWCNTs were easily accumulated with each other and hardly dispersed in water, and even in ethanol. After treatment by strong acid and sonication, the tube-like structure of the MWCNTs was well maintained, with a diameter of 10–50 nm and a length of several micrometers (Fig. 1b, c). The acid-treated MWCNTs could be stably suspended in deionized water over several months. Figure 1d presents the size distribution of the MWCNTs dispersed in water, from which the average hydrodynamic size was calculated as 171.6 nm with a polydispersity index of 0.179. Zeta potential measurement revealed a surface potential of about −56.5 mV, implying that a large number of carboxyl or hydroxyl groups were introduced in the process of acid oxidization. The FT-IR spectra (Fig. 2) confirmed the existence of the carboxyl groups, which appeared at 1712 cm^{-1}. The results of atomic absorption spectra revealed that the metal impurities were removed from the purified MWCNTs (wt%Mg <0.005%, wt%Co <0.005%). Although the treated MWCNTs had a large number of carboxylic groups with a negative surface charge, its dispersion with a concentration of 100 μg/mL in PBS or culture medium brought a neglectable change of pH value (<0.1) of the solution.

Influences of MWCNTs on Cell Viability

MTT reduction assay was used to investigate the cytotoxic effect of the MWCNTs on the human dermal fibroblasts and NIH 3T3 cells. It has been reported

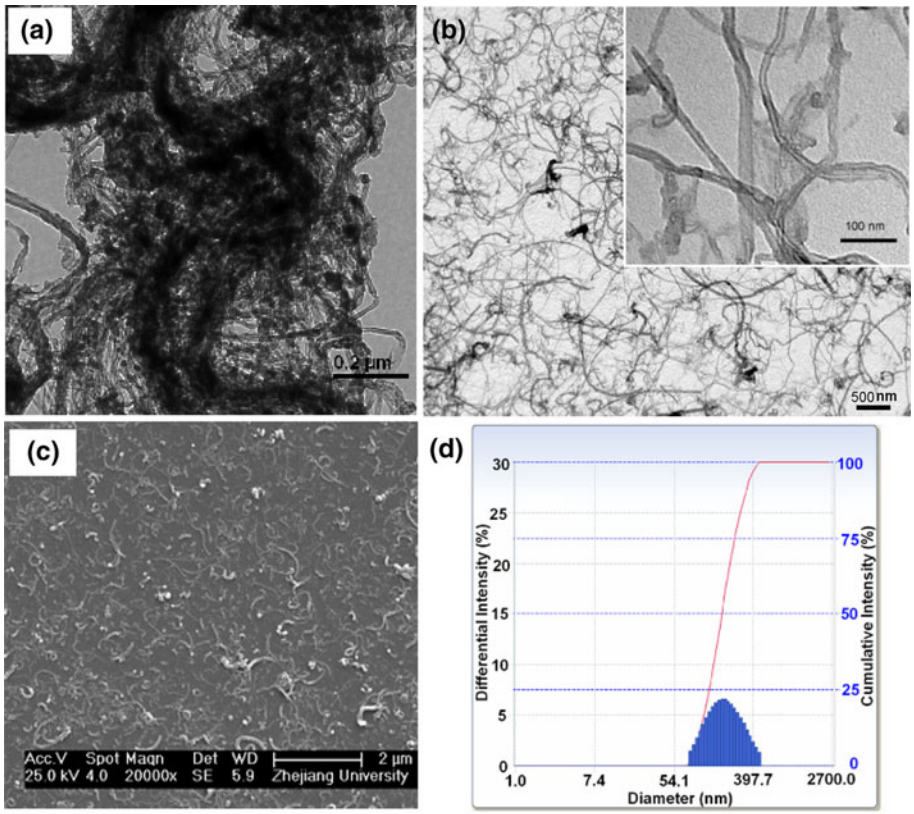

FIGURE 1. Typical TEM images of (a) pristine MWCNTs and (b) acid-treated MWCNTs. Inset of (b) is a magnified image. (c) SEM image and (d) DLS analysis of acid-treated MWCNTs in a dry state and in aqueous solution, respectively.

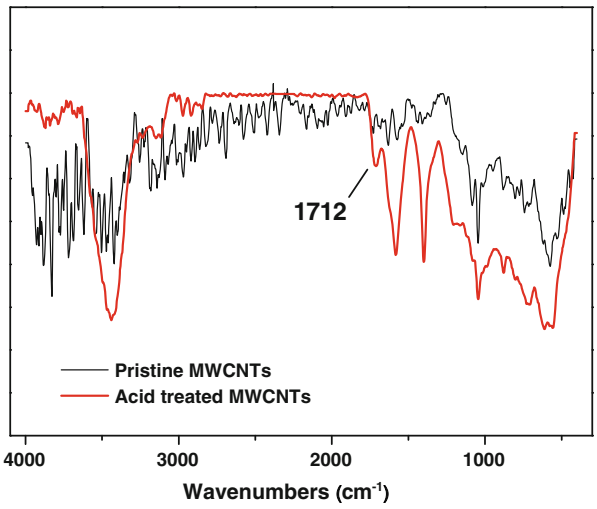

FIGURE 2. FT-IR spectra of pristine MWCNTs and acid-treated MWCNTs.

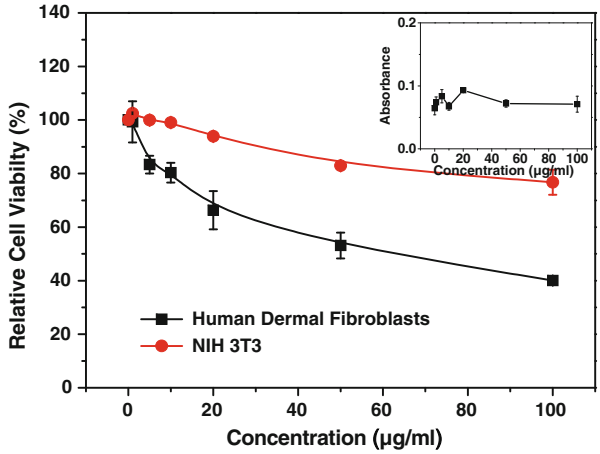

FIGURE 3. Relative viability of 3T3 cells and human dermal fibroblasts in the presence and absence of MWCNTs. The cells were incubated with MWCNTs of different concentrations (1, 5, 10, 20, 50, and 100 μg/mL) at 37 °C for 24 h. The viability of the control sample was set as 100%. *Inset*: effects of MWCNTs on the MTT dyes. MWNTs were treated with the MTT dyes without cells at the same concentrations for the same time periods.

that some types of NPs may bind to or react with MTT, leading to interference of toxicity assays.[24] However, the MWCNTs wound not react with MTT. Before using the MTT assay to detect the cell viability, control experiments were performed with corresponding concentrations of MWCNTs, finding no interference on the MTT assay (Fig. 3 inset). The study performed by Cheng *et al.* also approved this feasibility.[5]

As shown in Fig. 3, after culture with different concentrations of MWCNTs for 24 h, there was a significant dose-dependent decrease in viability with increasing dose of the MWCNTs for both types of fibroblasts. However, the MWCNTs had shown higher cytotoxicity to human fibroblasts than to NIH 3T3 fibroblasts, indicating that the human dermal fibroblasts are more sensitive to the MWCNTs stimulation.

Cell Cycle Analysis

We used fluorescence-activated cell sorting (FACS) analysis to study the cell cycle distribution of propidium iodide-stained cells treated with different concentrations of MWCNTs. The results are shown in Fig. 4 and Table 2. Along with increasing dose of the MWCNTs, more cells were found in the G1 phase and a fewer cells were found in the S phase and G2/M phase, regardless of the type of the fibroblasts. For example, after incubation with 50 μg/mL MWCNTs for 24 h the cell number in the G1 phase increased for about 16 and 13% for the 3T3 cells and human dermal fibroblasts, respectively.

Cell Adhesion and Real-Time RT-PCR Analysis

The adhesive ability of the MWCNTs-treated cells was quantified by comparing the MWCNTs-treated adhesive cell number to the control adhesive cell number. As shown in Fig. 5, the morphologies, attachment, and spreading behavior of the MWCNTs-treated cells were different from the untreated control cells. Compared to the normal spindle-shaped morphology of the control cells, the cells treated with the MWCNTs were less elongated and even became round. Black dots appeared in the cytoplasm of most cells, indicating cellular uptake of the MWCNTs. The cells attached for 24 h and the adherent cells were quantitated by counting in 12 different areas under an optical microscope (Fig. 5g). As a result, for the 3T3 cells incubated with 20 and 50 μg/mL MWCNTs, relative percentages of adherent cells were found to be about 77 and 55% of the control, respectively. For the human dermal fibroblasts, the relative percentages decreased to 77 and 59% of the control, respectively.

The real-time RT-PCR found that the MWCNTs treatment (50 μg/mL, 24 h) caused significantly decrease in the mRNA level of fibronectin (35%), laminin (28%), and FAK (39%) in human dermal fibroblasts ($p < 0.05$) too (Fig. 6).

Transwell Assay

To investigate the effect of the MWCNTs on cell migration, the migration ability of the fibroblasts was evaluated by using Millicell separate culture plate inserts. Figure 7 shows that the human dermal fibroblasts and 3T3 cells migrated through the filter of

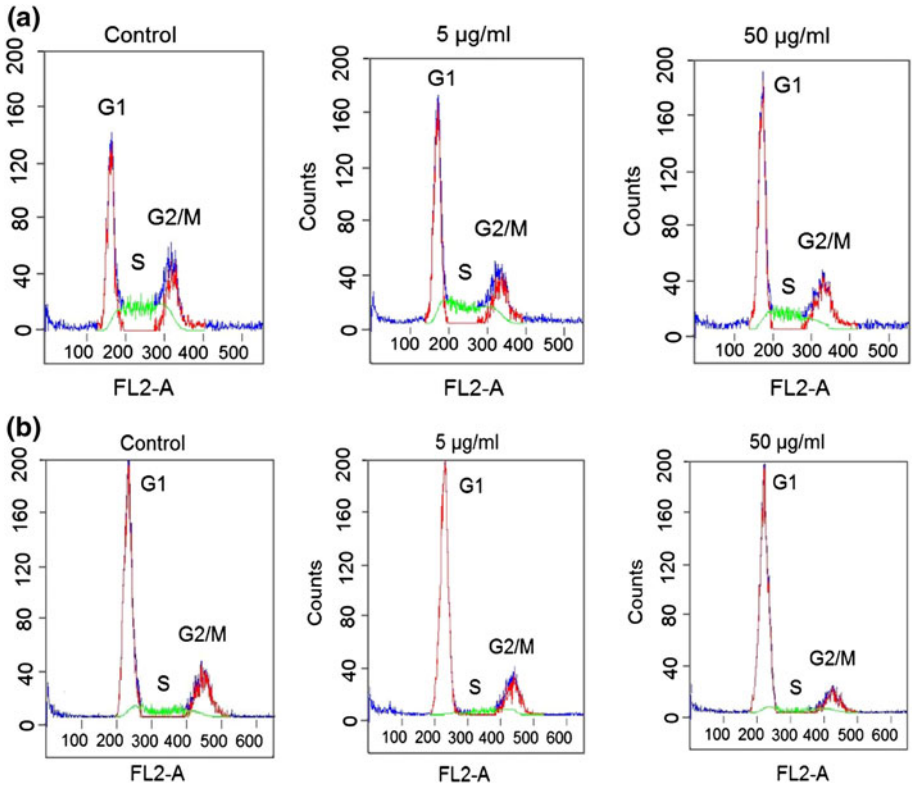

FIGURE 4. Cell cycle analysis of (a) 3T3 cells and (b) human dermal fibroblasts determined by flow cytometry. The cells were incubated without and with MWCNTs of a concentration of 5, 50 μg/mL at 37 °C for 24 h, respectively.

TABLE 2. Quantitative analysis of the cell cycle distribution.

Cell	Sample	G1 (%)	S (%)	G2/M (%)
NIH 3T3	Control	42.3 ± 1.9	35.0 ± 1.1	22.7 ± 0.9
	5 μg/mL MWCNTs	50.2 ± 2.4*	29.9 ± 0.7*	19.5 ± 1.2*
	50 μg/mL MWCNTs	58.0 ± 0.3*	24.2 ± 0.5*	17.8 ± 0.2*
Human dermal fibroblasts	Control	69.3 ± 3.1	12.0 ± 0.4	18.7 ± 2.7
	5 μg/mL MWCNTs	76.9 ± 2.8*	6.5 ± 0.2*	16.6 ± 2.6
	50 μg/mL MWCNTs	82.5 ± 2.6*	4.0 ± 0.2*	13.5 ± 2.4

* Indicates significant difference at $p < 0.05$ vs. control sample.

transwell chamber. As quantitatively depicted in Fig. 7g, the cell migration was significantly affected by the MWCNTs treatment regardless of the type of the fibroblasts.

The Wound Healing Assay and Stress Fiber Formation

In order to study whether the MWCNTs influence the wound healing process, the fibroblasts were exposed to different concentrations of MWCNTs for 24 h, and then scratched to form a linear wound. The process of wound closure was observed over the following 72 h. As shown in Fig. 8, the untreated cells migrated into and recovered the exposed surface within a shorter time period than the cells treated with the MWCNTs. Wound closure of the control cells almost finished at 48 and 72 h after initial wounding for the human dermal fibroblasts and 3T3 cells, respectively. However, the cells treated with 100 μg/mL MWCNTs moved more slowly and needed much longer closure time. Figure 8c shows the fluorescence image of FDA stained cells after wound closure for 72 h. It shows more clearly that the control cells arrayed orderly while the cells treated with the MWCNTs were much sparser and arranged stochastically. Quantitative analysis found that the wound healing degree was progressively decreased along with the increase of the MWCNTs concentration (data above the images). Particularly, when the cells were treated with 100 μg/mL MWCNTs, the healing degrees were only

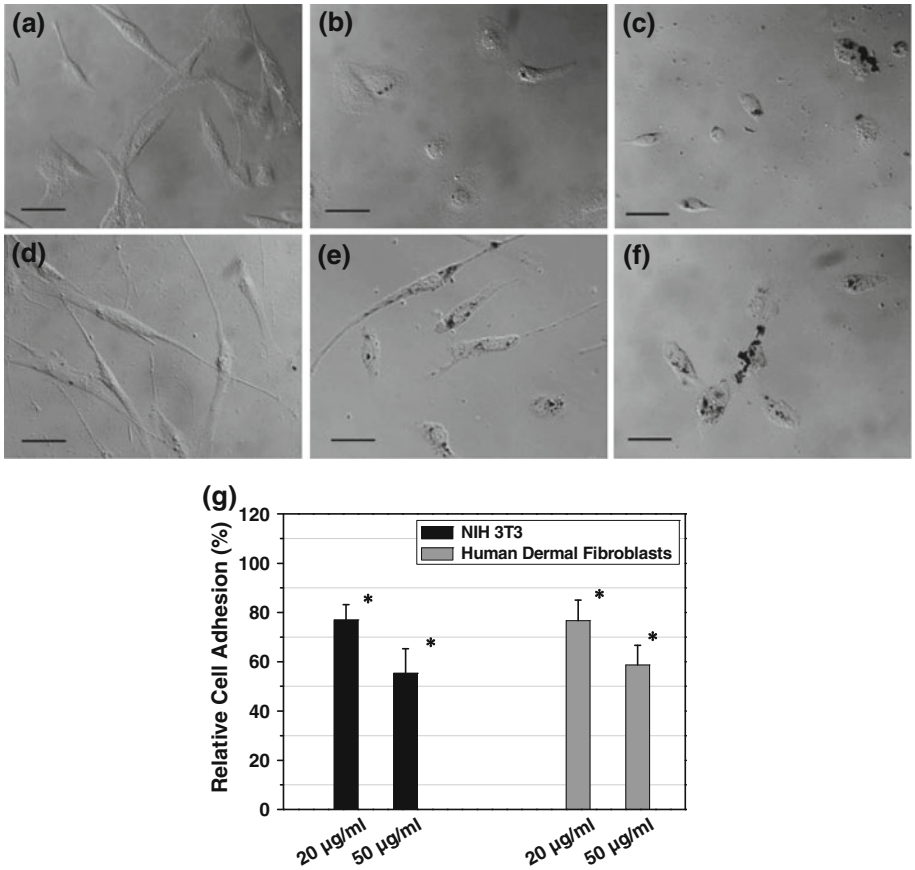

FIGURE 5. Morphologies of (a, b, c) 3T3 cells and (d, e, f) human dermal fibroblasts observed by using an optical microscope. Scale bar = 50 μm. The cells were incubated (a, d) without or with (b, e) 20 μg/mL and (c, f) 50 μg/mL of MWCNTs for 24 h, respectively, then detached, and then seeded to the culture plate with equal number and allowed to adhere for another 24 h. (g) Quantitative analysis of the cell adhesion from the images as shown in (a–f). The data were normalized to that of the control. Asterisk indicates significant difference at $p < 0.05$.

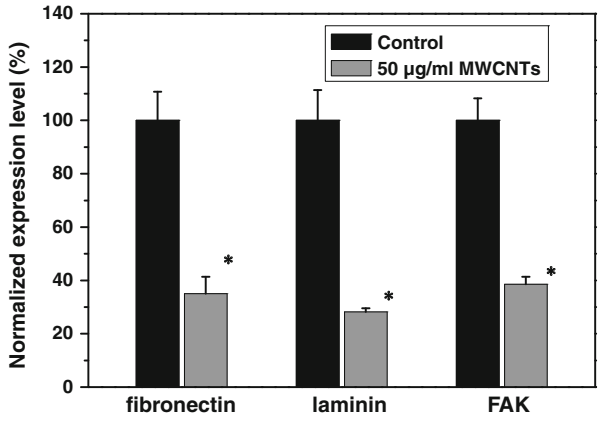

FIGURE 6. Real-time quantitative RT-PCR for the gene expression of fibronectin, laminin and FAK in human dermal fibroblasts in the presence and absence of MWCNTs. The data were normalized to that of the control. Asterisk indicates significant difference at $p < 0.05$.

47.0 and 11.7% for the 3T3 cells and human dermal fibroblasts, respectively, both are far smaller than that (>95%) of the controls of both fibroblasts.

F-actin staining was performed to examine the effects of MWCNTs on the cytoskeleton of human dermal fibroblasts and 3T3 cells. Figure 9 shows that the stress fibers in the control cells at the wound edge were well ordered and orientated parallel to the direction of cell migration, while the stress fibers in the cells treated with the MWCNTs decreased and became disordered.

DISCUSSION

Because of their geometry and hydrophobic surface, the pristine CNTs are not well soluble or dispersible in water. Previous studies have shown that the combine treatment by oxidization and sonication in strong acid produces short CNTs of high purity with carboxyl groups on the side walls and ends of the tubes.[21,37] The produced carboxyl groups impart hydrophilicity to the nanotubes and can couple simultaneously biomolecules such as oligonucleotides or proteins in order to achieve functional modifications.[21] According to the

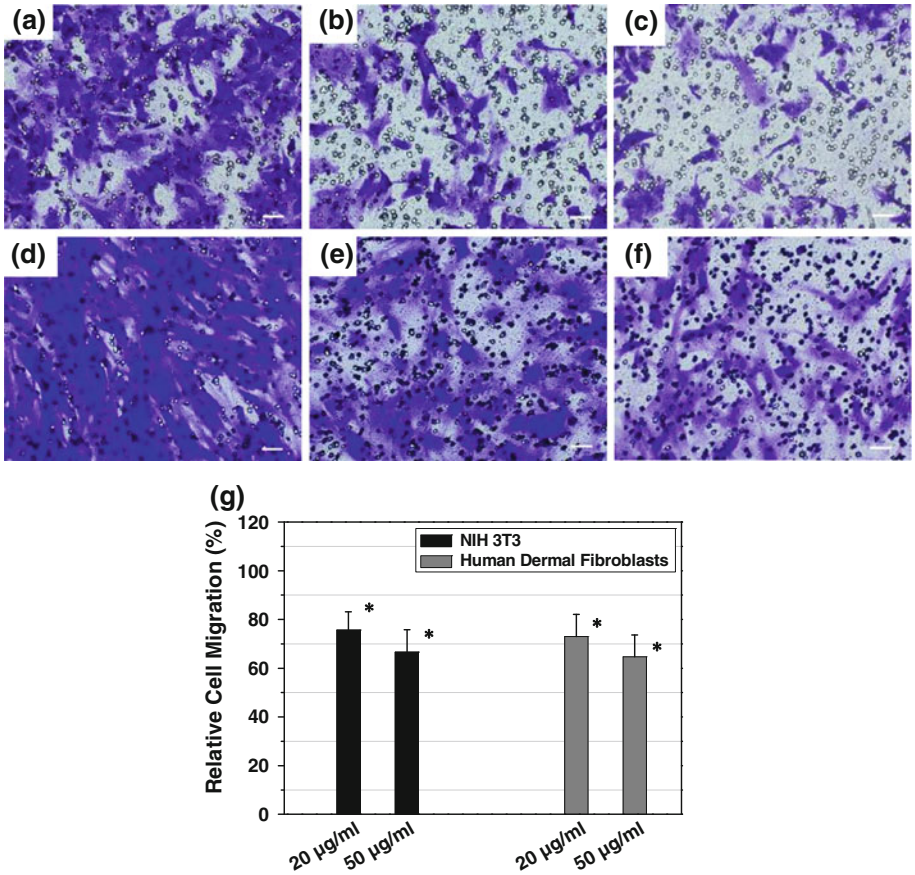

FIGURE 7. Optical images of (a, b, c) 3T3 cells and (d, e, f) human dermal fibroblasts (purple color) that had crossed through the pores (the tiny round hollows in the images) of transwell chamber and stained by crystal violet. Scale bar = 50 μm. The cells were incubated (a, d) without or with (b, e) 20 μg/mL and (c, f) 50 μg/mL of MWCNTs for 24 h, respectively, detached, and then seeded to the upper chamber with a cell number of 5×10^4 and incubated for another 10 h. (g) Quantitative analysis of the cell migration from the images as shown in (a–f). The data were normalized to that of the control. Asterisk indicates significant difference at $p < 0.05$ vs. control sample.

results of TEM and DLS, the tube-like structure of the MWCNTs was well maintained and the purified MWCNTs could be stably suspended in aqueous solution.

Ding *et al.*[8] and Patlolla *et al.*[35] demonstrated that the MWCNTs exposure caused strong cytotoxicity on human skin fibroblasts. In our study, we also observed a significant dose-dependent decrease in cell viability along with the increase of MWCNTs for both human fibroblasts and NIH 3T3 mouse fibroblasts. However, the human dermal fibroblasts are more susceptible to the MWCNTs stimulation. Intrinsic reasons for this phenomenon need to be clarified, although previously the slower population doubling time of the human fibroblasts is partially responsible.[4]

The cell cycle consists of interphases (G1, S, and G2) and mitosis (M). During the G1 period, the cells increase in size, produce RNA, and synthesize proteins for DNA formation. At the S phase DNA replication occurs, and the cells continue to grow, producing new proteins at the G2 phase. Nuclear and cytoplasmic division complete at the M stage.[31] According to the results of FACS analysis illustrated in Fig. 4 and Table 2, the cell cycle was blocked at the G1/S boundary and arrested in the G1 phase, indicating that DNA synthesis was impaired by the MWCNTs treatment.

Cell adhesion is an interaction between focal adhesion proteins and extracellular matrix or neighbor cells. It plays an important role in a range of cellular functions including cell migration, proliferation, differentiation, and tissue organization. Therefore, a quantitative analysis of cell adhesion ability is necessary to understand the effect of nanomaterials on cellular physiological functions. As illustrated in Fig. 5, the cells treated with the MWCNTs were less elongated and even became round compared with the spindle-shaped morphology of the control cells. Quantitative analysis indicated significant decrease of the adhesive cell number after exposed to 20 μg/mL MWCNTs for 24 h. These results are consistent with the previous report by Kaiser *et al.* that the mesothelioma cells

MSTO-211H incubated with the SWCNTs exhibited a weaker adherence than the control cells.[19] In order to explore the molecular mechanism of the weakened cell adhesion, real-time RT-PCR was performed to examine the expression profiles of adhesion specific genes, i.e., fibronectin, laminin, and FAK. The fibronectin and laminin are two important extracellular matrix glycoproteins that play major roles in cell adhesion, spreading, migration, and differentiation. Moreover, the fibronectin is also important for physiological processes such as wound healing and embryonic development.[6,33] FAK is an intracellular kinase localizing to focal adhesions, which regulates both cellular adhesion and antiapoptotic survival signaling.[49] The results of real-time RT-PCR indicated that the MWCNTs treatment caused significant decrease in the mRNA level of fibronectin, laminin, and FAK in human dermal fibroblasts. Cui *et al.*[7] and Tian *et al.*[46] used western blot to investigate the protein expression change of HEK293 cells and human fibroblasts caused by SWCNTs exposure, respectively. At the level of protein they found that the expression of fibronectin, laminin, and FAK decreased gradually as the culture time and the amount of SWCNTs increased, which is in agreement with our results. Their explanation are that the SWCNTs insert ruffles of the cell membranes, disturb the surface protein acceptors and activate extra cellular matrix protein signals. Consequently, the cell starts regulating the expressions levels of related genes and changing the cytoskeleton. Afterward, a displacement of internal organelles and a deformation of cell membrane take place, and thereon disturb cell adhesion and spreading. In our study, the similar mechanism should be applied, since the MWCNTs are structurally similar as the SWCNTs in terms of cellular interaction.

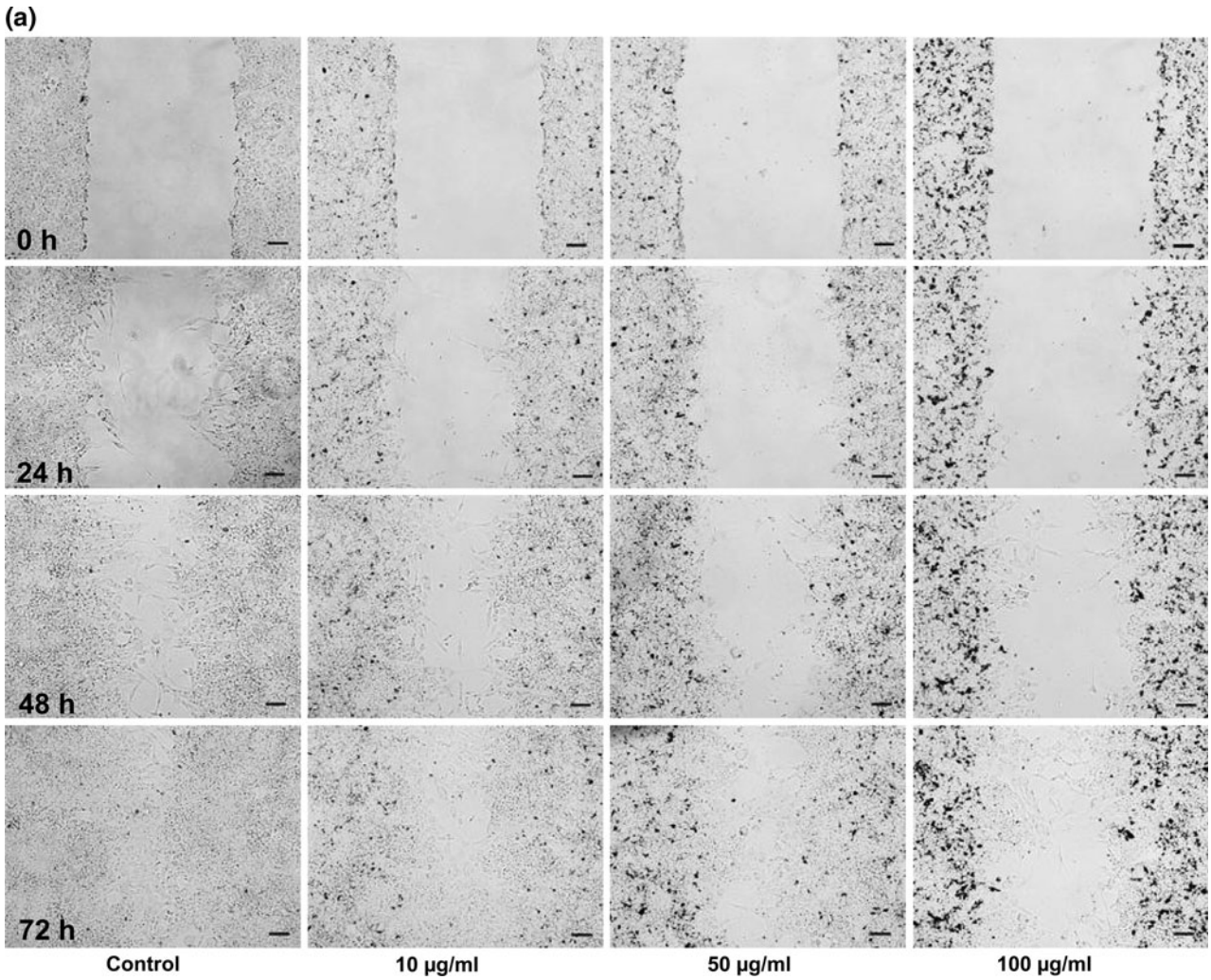

FIGURE 8. The wound healing process of (a) 3T3 cells and (b) human dermal fibroblasts observed by an optical microscope. (c) The fluorescence images of 3T3 cells (the upper panel) and human dermal fibroblasts (the lower panel) after wound closure for 72 h. The cells were stained with FDA, and the data above the images represent the wound healing degree. The cells were incubated without or with 10, 50 and 100 μg/mL of MWCNTs for 24 h before scratching, respectively. Scale bar = 100 μm.

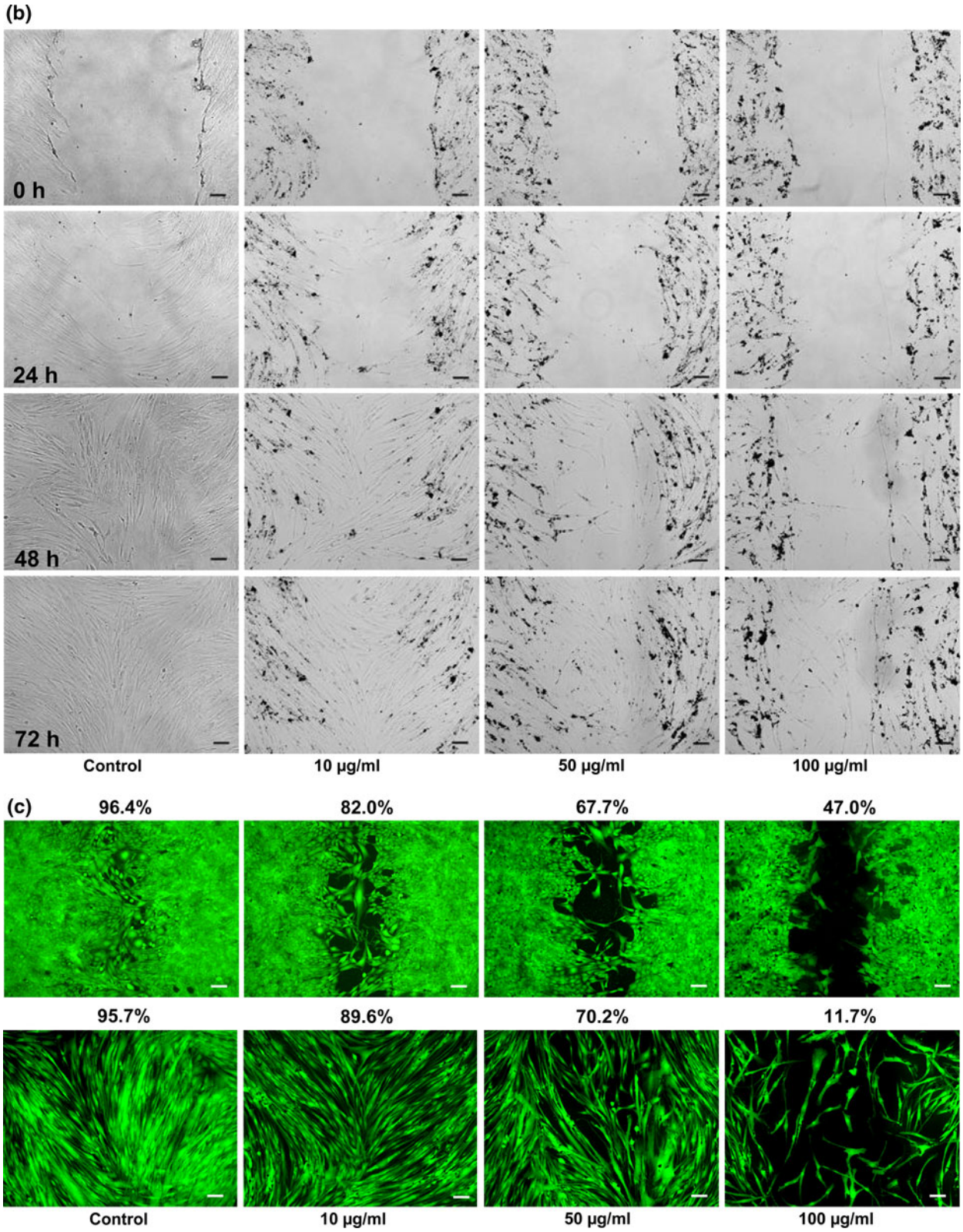

FIGURE 8. Continued.

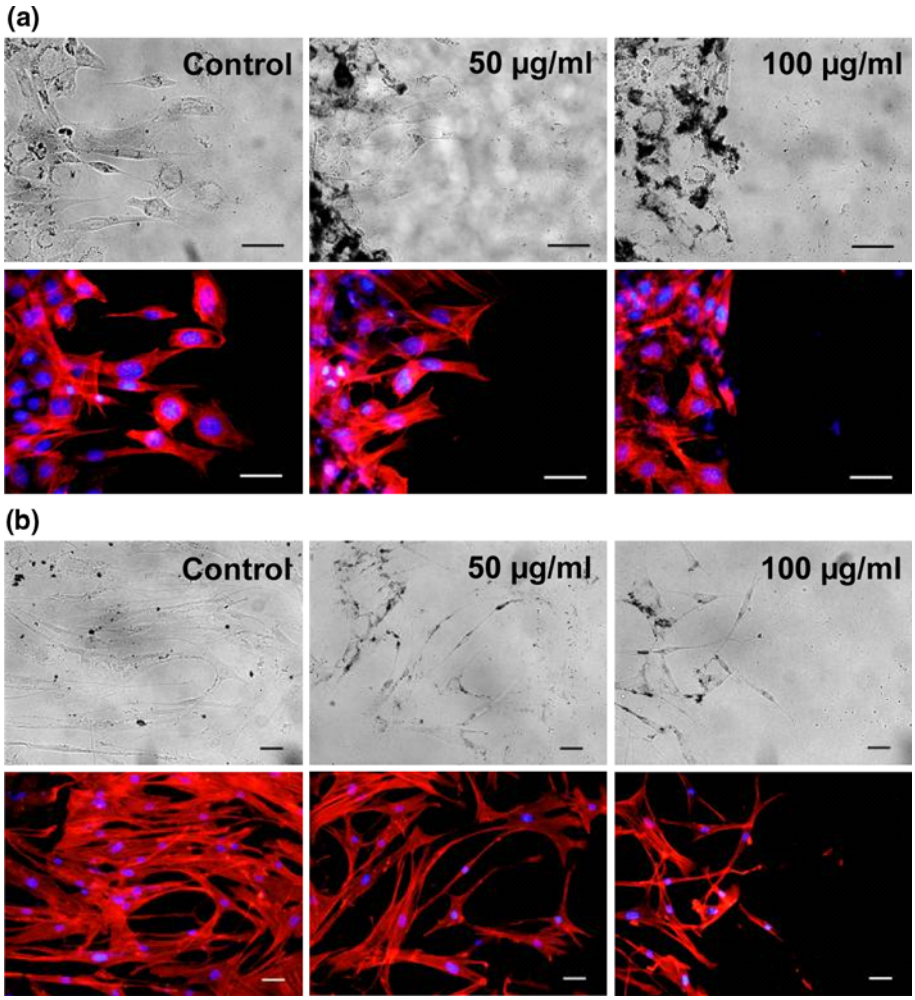

FIGURE 9. Cytoskeleton organization of (a) 3T3 cells and (b) human dermal fibroblasts treated without or with 50, 100 μg/mL of MWCNTs, respectively, at the wound edge 24 h after scratching. Upper, phase-contrast images; lower, fluorescence images. The F-actin was stained by rhodamine-conjugated phalloidin and the cell nuclei were stained by DAPI. Scale bar = 50 μm.

Cell migration participates in a variety of physiological and pathological processes such as embryonic development, cancer metastasis, blood vessel formation and remolding, tissue regeneration, immune surveillance, and inflammation.[9] Migration of the fibroblasts plays a central role in the wound healing process. In the initial period after injury, the fibroblasts from neighboring tissue proliferate and migrate into the wound area. Subsequently, they become the main cells that lay down the collagen matrix in the wound site,[44] and then keratinocytes differentiate and migrate across the wound bed.[32] According to the results of transwell assay and wound healing assay in this study, the migration ability of both the two kinds of fibroblasts were greatly impaired after MWCNTs treatment. Figure 8 indicates that with the increasing concentration of MWCNTs, the denuded area increased and the fibroblasts became much sparser and arranged stochastically. The inhibition of DNA replication and cell proliferation is believed to be one of the responsible reasons too since the wound healing process involves both cell proliferation and migration.

One of the important factors in regulating cell migration is the architecture of the cytoskeleton.[12] The cell migration is a complex cellular behavior resulted from the coordinated changes of the actin cytoskeleton, and the controlled formation and dispersal of cell adhesion sites.[48] The actin cytoskeleton, which is associated with protruding cellular structures such as filopodia and lamellipodia that form at the front of migrating cells,[43] in fibroblasts always exhibit as filaments. They are bundled into stress fibers which anchor within focal contacts at the cell periphery. Not only control over the cell morphology and migration, the cytoskeleton has also been found to be related with cell proliferation, mitosis, differentiation, and gene expression.[47] As previously reported, internalization of particles may disrupt cytoskeleton by forming vacuoles

in the cell body.[10,13] Therefore, F-actin staining was performed to examine the effects of the MWCNTs on the cytoskeleton of human dermal fibroblasts and 3T3 cells. According to the results presented in Fig. 9, the actin fibrils were disturbed and the stress fibers decreased after treatment with the MWCNTs, which may be the major cause of the impedance of cell proliferation, adhesion, and migration.[36] It has been reported that coating with layers of biocompatible polymer would decrease the toxicity of nanoparticles to cells and tissues.[27,32] Furthermore, functionalization of the CNTs with biopolymers such as proteins is emerging as a promising way to expanding their biomedical applications. In the serum-containing culture medium, non-specific adsorption of proteins on the MWCNTs took place too (75 ± 10 μg proteins/mg MWCNTs after 6 h incubation, as detected by BCA assay). Although it is not clear if the MWCNTs were fully covered by the proteins, we believe that the one-dimensional shape or the nature of small size of the MWCNTs is still the main reason. Whether the surface modification can really reduce the adverse effects of the CNTs to organisms especially the physiological functions of cells is still uncertain.

CONCLUSION

In the present study, the adverse effects of acid-treated MWCNTs on NIH 3T3 cells and human dermal fibroblasts were explored. The presence of the MWCNTs was responsible for the down-regulated expression level of adhesion-related genes and abnormal actin filaments, and thereby affected the physiological functions of the cells in terms of cell proliferation, mitosis, adhesion, and migration.

ACKNOWLEDGMENTS

This work is financially supported by the Natural Science Foundation of China (50903069, 50873087), Zhejiang Provincial Natural Science Foundation of China (Z4090177) and Frame Work Program 7 of European Commission (FP7-NMP-SMALL-2).

REFERENCES

[1]Baughman, R. H., A. A. Zakhidov, and W. A. de Heer. Carbon nanotubes—the route toward applications. *Science* 297(5582):787–792, 2002.

[2]Bianco, A., and M. Prato. Can carbon nanotubes be considered useful tools for biological applications? *Adv. Mater.* 15(20):1765–1766, 2003.

[3]Bottini, M., S. Bruckner, K. Nika, N. Bottini, S. Bellucci, A. Magrini, A. Bergamaschi, and T. Mustelin. Multi-walled carbon nanotubes induce T lymphocyte apoptosis. *Toxicol. Lett.* 160(2):121–126, 2006.

[4]Chang, J. S., K. L. Chang, D. F. Hwang, and Z. L. Kong. In vitro cytotoxicitiy of silica nanoparticles at high concentrations strongly depends on the metabolic activity type of the cell line. *Environ. Sci. Technol.* 41(6):2064–2068, 2007.

[5]Cheng, C., K. H. Muller, K. K. Koziol, J. N. Skepper, P. A. Midgley, M. E. Welland, and A. E. Porter. Toxicity and imaging of multi-walled carbon nanotubes in human macrophage cells. *Biomaterials* 30(25):4152–4160, 2009.

[6]Colognato, H., and P. D. Yurchenco. Form and function: the laminin family of heterotrimers. *Dev. Dyn.* 218(2): 213–234, 2000.

[7]Cui, D. X., F. R. Tian, C. S. Ozkan, M. Wang, and H. J. Gao. Effect of single wall carbon nanotubes on human HEK293 cells. *Toxicol. Lett.* 155(1):73–85, 2005.

[8]Ding, L., J. Stilwell, T. Zhang, O. Elboudwarej, H. Jiang, J. P. Selegue, P. A. Cooke, J. W. Gray, and F. F. Chen. Molecular characterization of the cytotoxic mechanism of multiwall carbon nanotubes and nano-onions on human skin fibroblast. *Nano Lett.* 5(12):2448–2464, 2005.

[9]Even-Ram, S., and K. M. Yamada. Cell migration in 3D matrix. *Curr. Opin. Cell. Biol.* 17(5):524–532, 2005.

[10]Fujimoto, L. M., R. Roth, J. E. Heuser, and S. L. Schmid. Actin assembly plays a variable, but not obligatory role in receptor-mediated endocytosis in mammalian cells. *Traffic* 1(2):161–171, 2000.

[11]Gao, H. J., Y. Kong, and D. X. Cui. Spontaneous insertion of DNA oligonucleotides into carbon nanotubes. *Nano Lett.* 3(4):471–473, 2003.

[12]Gotlieb, A. I. The endothelial cytoskeleton: organization in normal and regenerating endothelium. *Toxicol. Pathol.* 18(4 Pt 1):603–617, 1990.

[13]Gupta, A. K., M. Gupta, S. J. Yarwood, and A. S. Curtis. Effect of cellular uptake of gelatin nanoparticles on adhesion, morphology and cytoskeleton organisation of human fibroblasts. *J. Control Rel.* 95(2):197–207, 2004.

[14]Hafner, J. H., C. L. Cheung, A. T. Woolley, and C. M. Lieber. Structural and functional imaging with carbon nanotube AFM probes. *Prog. Biophys. Mol. Biol.* 77(1):73–110, 2001.

[15]Hu, H., Y. Ni, S. K. Mandal, V. Montana, B. Zhao, R. C. Haddon, and V. Parpura. Polyethyleneimine functionalized single-walled carbon nanotubes as a substrate for neuronal growth. *J. Phys. Chem. B* 109(10):4285–4289, 2005.

[16]Iijima, S. Helical microtubules of graphitic carbon. *Nature* 354:56–58, 1991.

[17]Jia, G., H. F. Wang, L. Yan, X. Wang, R. J. Pei, T. Yan, Y. L. Zhao, and X. B. Guo. Cytotoxicity of carbon nanomaterials: single-wall nanotube, multi-wall nanotube, and fullerene. *Environ. Sci. Technol.* 39(5):1378–1383, 2005.

[18]Kagan, V. E., Y. Y. Tyurina, V. A. Tyurin, N. V. Konduru, A. I. Potapovich, A. N. Osipov, E. R. Kisin, D. Schwegler-Berry, R. Mercer, V. Castranova, and A. A. Shvedova. Direct and indirect effects of single walled carbon nanotubes on RAW 264.7 macrophages: role of iron. *Toxicol. Lett.* 165(1):88–100, 2006.

[19]Kaiser, J. P., P. Wick, P. Manser, P. Spohn, and A. Bruinink. Single walled carbon nanotubes (SWCNT) affect cell physiology and cell architecture. *J. Mater. Sci.* 19(4):1523–1527, 2008.

[20]Kaiser, J. P., H. F. Krug, and P. Wick. Nanomaterial cell interactions: how do carbon nanotubes affect cell physiology? *Nanomedicine* 4(1):57–63, 2009.
[21]Kam, N. W., and H. Dai. Carbon nanotubes as intracellular protein transporters: generality and biological functionality. *J. Am. Chem. Soc.* 127(16):6021–6026, 2005.
[22]Kisin, E. R., A. R. Murray, M. J. Keane, X. C. Shi, D. Schwegler-Berry, O. Gorelik, S. Arepalli, V. Castranova, W. E. Wallace, V. E. Kagan, and A. A. Shvedova. Single-walled carbon nanotubes: geno- and cytotoxic effects in lung fibroblast V79 cells. *J. Toxicol. Environ. Health A* 70(24): 2071–2079, 2007.
[23]Kostarelos, K., L. Lacerda, G. Pastorin, W. Wu, S. Wieckowski, J. Luangsivilay, S. Godefroy, D. Pantarotto, J. P. Briand, S. Muller, M. Prato, and A. Bianco. Cellular uptake of functionalized carbon nanotubes is independent of functional group and cell type. *Nat. Nanotechnol.* 2(2): 108–113, 2007.
[24]Laaksonen, T., H. Santos, H. Vihola, J. Salonen, J. Riikonen, T. Heikkila, L. Peltonen, N. Kurnar, D. Y. Murzin, V. P. Lehto, and J. Hirvonent. Failure of MTT as a toxicity testing agent for mesoporous silicon microparticles. *Chem. Res. Toxicol.* 20(12):1913–1918, 2007.
[25]Li, Y., X. B. Zhang, X. Y. Tao, J. M. Xu, W. Z. Huang, J. H. Luo, Z. Q. Luo, T. Li, F. Liu, Y. Bao, and H. J. Geise. Mass production of high-quality multi-walled carbon nanotube bundles on a Ni/Mo/MgO catalyst. *Carbon* 43(2):295–301, 2005.
[26]Manna, S. K., S. Sarkar, J. Barr, K. Wise, E. V. Barrera, O. Jejelowo, A. C. Rice-Ficht, and G. T. Ramesh. Single-walled carbon nanotube induces oxidative stress and activates nuclear transcription factor-kappaB in human keratinocytes. *Nano Lett.* 5(9):1676–1684, 2005.
[27]Mao, Z. W., B. Wang, L. Ma, C. Y. Gao, and J. C. Shen. The influence of polycaprolactone coating on the internalization and cytotoxicity of gold nanoparticles. *Nanomedicine* 3(3):215–223, 2007.
[28]Monteiro-Riviere, N. A., and A. O. Inman. Challenges for assessing carbon nanomaterial toxicity to the skin. *Carbon* 44(6):1070–1078, 2006.
[29]Monteiro-Riviere, N. A., A. O. Inman, Y. Y. Wang, and R. J. Nemanich. Surfactant effects on carbon nanotube interactions with human keratinocytes. *Nanomedicine* 1(4):293–299, 2005.
[30]Oberlin, A., M. Endo, and T. Koyama. Filamentous growth of carbon through benzene decomposition. *J. Cryst. Growth* 32(3):335–349, 1976.
[31]Oh, J. M., S. J. Choi, S. T. Kim, and J. H. Choy. Cellular uptake mechanism of an inorganic nanovehicle and its drug conjugates: enhanced efficacy due to clathrin-mediated endocytosis. *Bioconjug. Chem.* 17(6):1411–1417, 2006.
[32]Pan, Z., W. Lee, L. Slutsky, R. A. Clark, N. Pernodet, and M. H. Rafailovich. Adverse effects of titanium dioxide nanoparticles on human dermal fibroblasts and how to protect cells. *Small* 5(4):511–520, 2009.
[33]Pankov, R., and K. M. Yamada. Fibronectin at a glance. *J. Cell. Sci.* 115(20):3861–3863, 2002.
[34]Pantarotto, D., R. Singh, D. McCarthy, M. Erhardt, J. P. Briand, M. Prato, K. Kostarelos, and A. Bianco. Functionalized carbon nanotubes for plasmid DNA gene delivery. *Angew. Chem. Int. Ed.* 43(39):5242–5246, 2004.
[35]Patlolla, A., B. Patlolla, and P. Tchounwou. Evaluation of cell viability, DNA damage, and cell death in normal human dermal fibroblast cells induced by functionalized multiwalled carbon nanotube. *Mol. Cell Biochem.* 331: 207–214, 2009.
[36]Pernodet, N., X. Fang, Y. Sun, A. Bakhtina, A. Ramakrishnan, J. Sokolov, A. Ulman, and M. Rafailovich. Adverse effects of citrate/gold nanoparticles on human dermal fibroblasts. *Small* 2(6):766–773, 2006.
[37]Raja, P. M., J. Connolley, G. P. Ganesan, L. Ci, P. M. Ajayan, O. Nalamasu, and D. M. Thompson. Impact of carbon nanotube exposure, dosage and aggregation on smooth muscle cells. *Toxicol. Lett.* 169(1):51–63, 2007.
[38]Reddy, A. R., Y. N. Reddy, D. R. Krishna, and V. Himabindu. Multi wall carbon nanotubes induce oxidative stress and cytotoxicity in human embryonic kidney (HEK293) cells. *Toxicology* 272(1–3):11–16, 2010.
[39]Ridley, A. J., M. A. Schwartz, K. Burridge, R. A. Firtel, M. H. Ginsberg, G. Borisy, J. T. Parsons, and A. R. Horwitz. Cell migration: integrating signals from front to back. *Science* 302(5651):1704–1709, 2003.
[40]Sayes, C. M., F. Liang, J. L. Hudson, J. Mendez, W. Guo, J. M. Beach, V. C. Moore, C. D. Doyle, J. L. West, W. E. Billups, K. D. Ausman, and V. L. Colvin. Functionalization density dependence of single-walled carbon nanotubes cytotoxicity in vitro. *Toxicol. Lett.* 161(2): 135–142, 2006.
[41]Schneider, M., F. Stracke, S. Hansen, and U. F. Schaefer. Nanoparticles and their interactions with the dermal barrier. *Dermatoendocrinology* 1(4):197–206, 2009.
[42]Shi, H., Y. Huang, H. Zhou, X. Song, S. Yuan, Y. Fu, and Y. Luo. Nucleolin is a receptor that mediates antiangiogenic and antitumor activity of endostatin. *Blood* 110(8): 2899–2906, 2007.
[43]Small, J. V., T. Stradal, E. Vignal, and K. Rottner. The lamellipodium: where motility begins. *Trends Cell Biol.* 12(3):112–120, 2002.
[44]Stadelmann, W. K., A. G. Digenis, and G. R. Tobin. Physiology and healing dynamics of chronic cutaneous wounds. *Am. J. Surg.* 176(2A Suppl):26S–38S, 1998.
[45]Tabet, L., C. Bussy, N. Amara, A. Setyan, A. Grodet, M. J. Rossi, J. C. Pairon, J. Boczkowski, and S. Lanone. Adverse effects of industrial multiwalled carbon nanotubes on human pulmonary cells. *J. Toxicol. Environ. Health A* 72(2):60–73, 2009.
[46]Tian, F. R., D. X. Cui, H. Schwarz, G. G. Estrada, and H. Kobayashi. Cytotoxicity of single-wall carbon nanotubes on human fibroblasts. *Toxicol. In Vitro* 20(7):1202–1212, 2006.
[47]Varedi, M., A. Ghahary, P. G. Scott, and E. E. Tredget. Cytoskeleton regulates expression of genes for transforming growth factor-beta 1 and extracellular matrix proteins in dermal fibroblasts. *J. Cell Physiol.* 172(2):192–199, 1997.
[48]Wehrle-Haller, B., and B. A. Imhof. Actin, microtubules and focal adhesion dynamics during cell migration. *Int. J. Biochem. Cell Biol.* 35(1):39–50, 2003.
[49]Xu, L. H., X. Yang, R. J. Craven, and W. G. Cance. The COOH-terminal domain of the focal adhesion kinase induces loss of adhesion and cell death in human tumor cells. *Cell Growth Differ.* 9(12):999–1005, 1998.
[50]Zhao, B., H. Hu, K. M. Swadhin, and R. C. Haddon. A bone mimic based on the self-assembly of hydroxyapatite on chemically functionalized single-walled carbon nanotubes. *Chem. Mater.* 17(12):3235–3241, 2005.